

# Actuator torque optimization of an automotive thermal management mechatronic valve based on a hydro-mechanical modelling and experimental validation

Montassar KHAMMASSI<sup>a</sup>, Bertrand BARBEDETTE<sup>a</sup>, Judicaël AUBRY<sup>a</sup>,  
Mickael CORMERAIS<sup>b</sup>, Chérif LAROUCI<sup>a</sup>, Fethi BENOUEZDOU<sup>c</sup>

a. ESTACA'LAB: École supérieure des techniques aéronautiques et de construction automobile,  
montassar.khammassi@estaca.fr

b. MANN+HUMMEL, mickael.cormerais@mann-hummel.com

c. LISV: Laboratoire d'Ingénierie des Systèmes de Versailles, fethi.benouezdou@uvsq.fr

## Abstract :

*Improving fuel economy and reducing the Greenhouse-Gas emissions have been the determining factors in the development and implementation of innovative automotive technologies. Engine thermal management is one of the research fields that tries to solve these issues. It can be applied when controlling temperatures in different cooling circuits with an electronically actuated valve, which respects certain thermal management strategies. This control varies depending on several parameters such as temperature, load and engine rotational speed. This paper is part of a larger work that aims to improve the robustness of this valve design process since the early steps while minimizing the torque requirements of the DC-actuator. The first part of the paper will describe the hydro-mechanical concept of the valve. The second part will be focused on the hydro-mechanical model that has been developed in order to simulate the multi-physical environment and so was validated based on available experimental measurements. The third part is concentrated on the model experimental validation. The last part is dedicated to discuss optimization results of a particle swarm based optimization (PSO) loop applied on a simpler model, which helps to determine an optimal geometrical configuration.*

**Key words: thermal management / mechatronic systems / numerical simulation / experimental validation / particle swarm based optimization (PSO)**

## 1 Introduction

The EIA (United States Energy Information Administration) estimates that world consumption of oil and other liquid fuels is 93,8 million barrels per day (Mb/d) for 2015 and expects this consumption to increase by 1,4 Mb/d in the next years to come [1]. Oil is the world's first energy resource as it satisfies 32% of energy needs. It is the most used energy resource in transportation with more than 90% of the final energy consumption (Figure 1).

Automotive manufacturers are currently searching for solutions to reduce engine emissions in order to improve fuel economy and satisfy global regulations, which set maximum limits for exhaust emissions

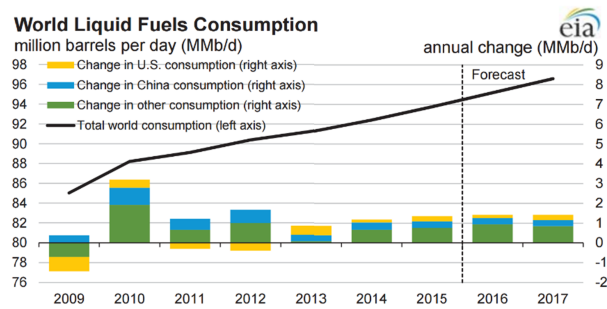


Figure 1: World oil consumption

of vehicles. Otherwise, they get a penalty for each gram of exceeded emissions per kilometer on each registered car [2]. Since many years, considerable improvements have been made by reducing the global weight of the vehicle, friction losses in the engine, aerodynamic drag on the body, rolling resistance of the tire/road interface or by trying new materials such as new metallic alloys or composite materials. In this paper, we are interested in engine thermal management, and more precisely, in coolant temperature control by an electronically controlled valve.

The oil temperature is directly linked to the coolant temperature. By increasing it, the oil viscosity is decreased, which is the key to reducing mechanical losses due to friction [4], [6], especially in the first moments from a cold start. This decreases the fuel consumption and so the  $CO_2$  emissions. In this context, MANN+HUMMEL (automotive component supplier in thermal management) has brought an innovative approach to one of the most important engine parts: the Active Cooling Thermo-Management Valve (ACT Valve). It represents a replacement for current wax-thermostat based cooling management systems. In fact, the electronically controlled 'smart' ACT Valve gives a new design to a traditional engine component which has always relied on wax thermostats (or calorstats), in order to control engine cooling [3]. Moreover, wax thermostats have the inevitable problem of slow response time, due to the time of wax thermal expansion, which has a direct effect on engine temperature regulation [7]. The ACT valve reduces fuel consumption by 1,6% on average [4]. So making engine run at a higher coolant temperature, in a short warm up time, ensures a significant decrease of fuel consumption. In addition, the "no flow" position of the ACT valve guarantees a fast warm up time. In fact, when the engine is cold, the "no flow" valve position allows the engine to warm up faster, by keeping all valves closed, as the vehicle reaches the optimum operating regime faster (Figure 2).

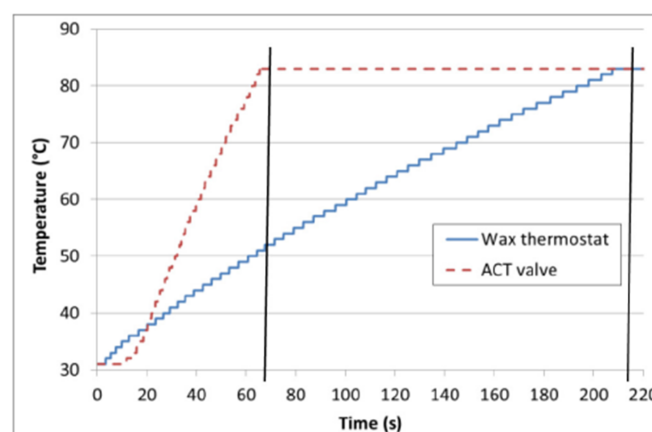


Figure 2: The "no flow" position effect of the ACT valve compared to wax thermostat [4]

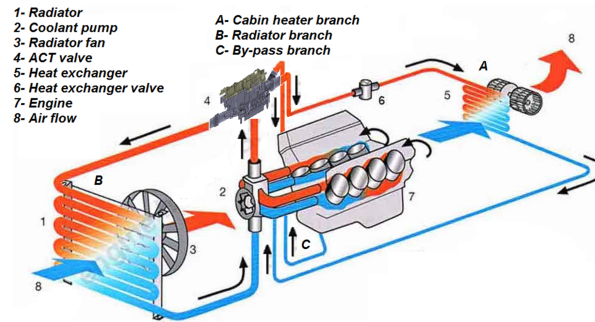


Figure 3: Typical external simplified coolant circuit

The ACT valve is located on the engine breach as part of the coolant circuit, which is composed generally of three branches: cabin heater, radiator and bypass (Figure 3). This last branch is used to increase the temperature in the warm up phase (after the "no flow" position) as the coolant flows from the engine to the pump and flows back to the engine again in a closed loop.

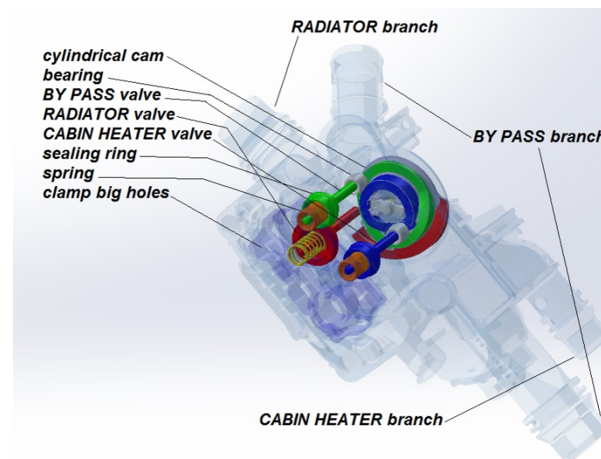


Figure 4: The ACT valve consisting internal parts

The ACT valve is mainly composed of a rotating cylindrical cam driving by a DC-actuator. It controls, accurately, the distribution and flow of the coolant in different branches of the cooling circuit including the engine and the interior heating/cooling system through valves that manage the opening and closing of branches (Figure 4).

This paper is part of a larger work that aims to improve the robustness of the ACT valve design process since the early steps while minimizing the torque requirements of the DC-actuator. Taking into account the multi-physical constraints of the operating environment such as water regain, mechanical load, fatigue, wear and clearances, but also of manufacturing constraints and process and geometrical tolerances related to the injection of thermoplastic parts. So in order to qualify the design process as robust, these uncertainties must be taken into account from the design phase to ensure the effectiveness and reliability of this valve over its lifetime. This paper deals with a new hydro-mechanical model, which is composed of four different sub-models, a mechanical model, a hydraulic model, and two local models of contact and wear. Modeling has been developed in order to simulate the multi-physical environment and so was validated based on experimental data. The most interesting parameter is the torque required for the cam rotation because its maximum value in full charge corresponds to the torque requirement of the DC-Actuator. Finally, an optimal geometrical configuration was determined, using a particle swarm based

optimization (PSO) process for which we have created a simpler model based on the global previous one.

## 2 Hydro-mechanical modeling

### 2.1 The global multi-physical model

In order to ensure the physical coupling between the mechanical model and the hydraulic model, the coolant flow generates a pressure drop when passing through the act valve. This pressure exerts a hydro-mechanical force on the projected area of the valve. Depending on the engine speed and load, the hydraulic forces can reach 80% of contribution in the torque requirements [4].

The hydraulic model gives as output the pressure drops of the three valves according to their positions given by the mechanical model (Figure 5). The engine rotational speed in RPM are also included since the engine is coupled to the coolant pump and as its the rotational speed increases, the pressure exerted by the coolant pump on the ACT valve is also increased.

The local wear model communicates with the mechanical model, as this last one gives as output the normal force exerted on top head of each valve, the wear model estimates the wear on the valve head and gives back new valve lift to the mechanical model. The modeling was based on the Global Incremental Wear Model (GIWM) [11], which relays on *Archard* theory of wear [12].

The local contact model is implemented in the mechanical model and takes as input the material properties and the geometrical aspects of the contact (e.g. sphere to plane in our case). The electrical actuator is modeled as a constant velocity source in which the inverse dynamics method is used to determine the resistive torque on the cam.

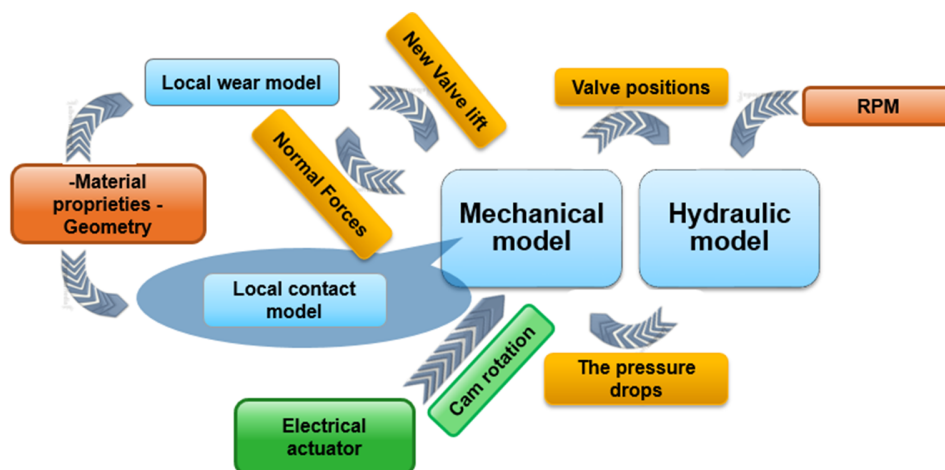


Figure 5: Flow chart for the global multi-physical model and its interactions

Both local wear and contact models presented here are going to be used in future works. This global multi-physical model was implemented and so was validated on available experimental data for a specific geometrical configuration of the ACT valve. The modeling was conducted on "Simscape Multibody" modeling environment. The multi-physical model was presented and its modeling equations were explained in our previous work [5].

*Note for readers: All results presented are normalized to the maximal value, due to confidential context.*

## 2.2 Model sensitivity analysis

To improve the performances of the act valve, we went to look for new configurations of parameters that could be interesting. Car manufacturer impose their hydraulic specifications and a maximal packaging constraints, these constraints orient us to dig more in the mechatronic aspects of the system. A sensitivity analysis was carried out on the global multi-physical model to evaluate the sensitivity of the torque requirements to certain geometric parameters such as the slopes of the cam profile, radius of the the curves, friction coefficients and the radius of the tracks of the cam also to the rotational speed of the engine.

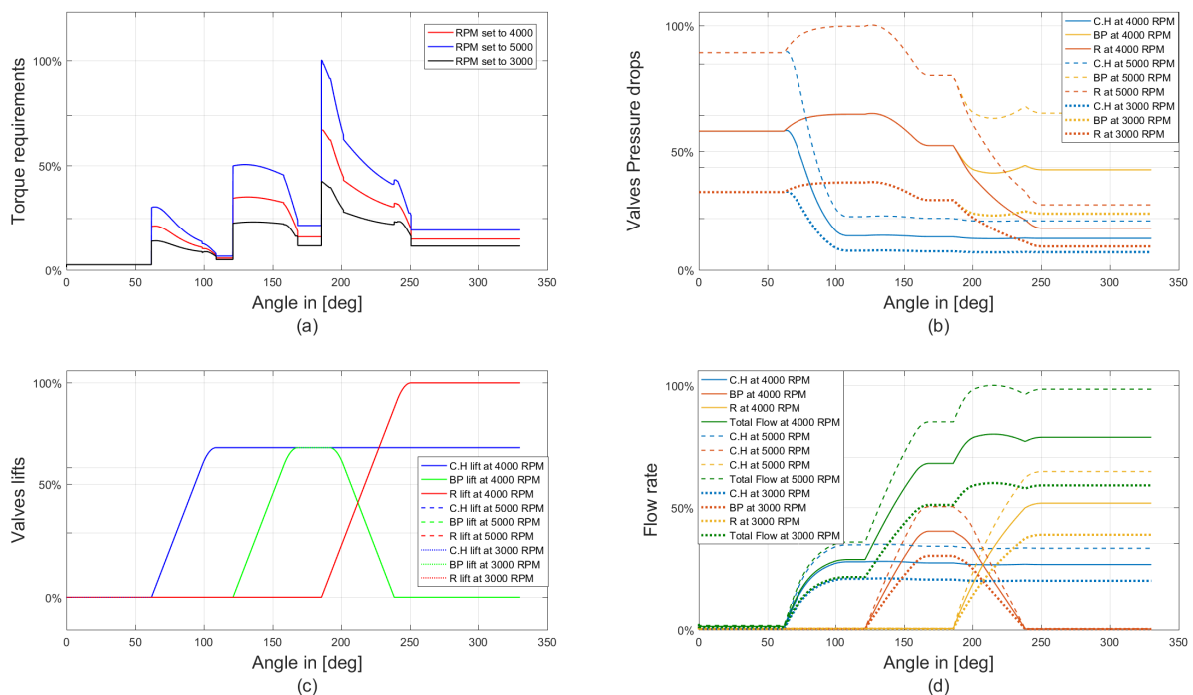


Figure 6: (a) resistive torque, (b) pressure drop, (c) lift and (d) flow rate sensitivity to RPM variation

### First example: Rotational Engine speed RPM

Increasing the engine speed from 3000 RPM to 5000 RPM causes an increase in the average torque and in the maximum torque which can rise by 60% (figure 6.a). This augmentation is directly related to the pressure drops created in the ACT valve. The increase in coolant flow through the ACT valve, as a result of this increase in RPM, is at the origin of these pressure drops.

### Second example: Cam profile angles

As shown on the figure 7.a, the total resistive torque, the valves lifts, the pressure drop and flow rate are all directly related to the rising angle of the cam. The reduction of the angle implies a reduction in the torque, it can reach 5% for a variation of just 4 deg. the reduction of the angle also implies an increase in the length of the contact zone of the cam on the valve while being limited by 330 deg. The reduction of the angle also implies an increase in the length of the contact zone between the cam and the valve while being limited by 330 deg.

Several sensitivity analysis were performed and many parameters were tested. System sensitivity analysis has provided a better understanding of the capacity and limitations of its performance, and will

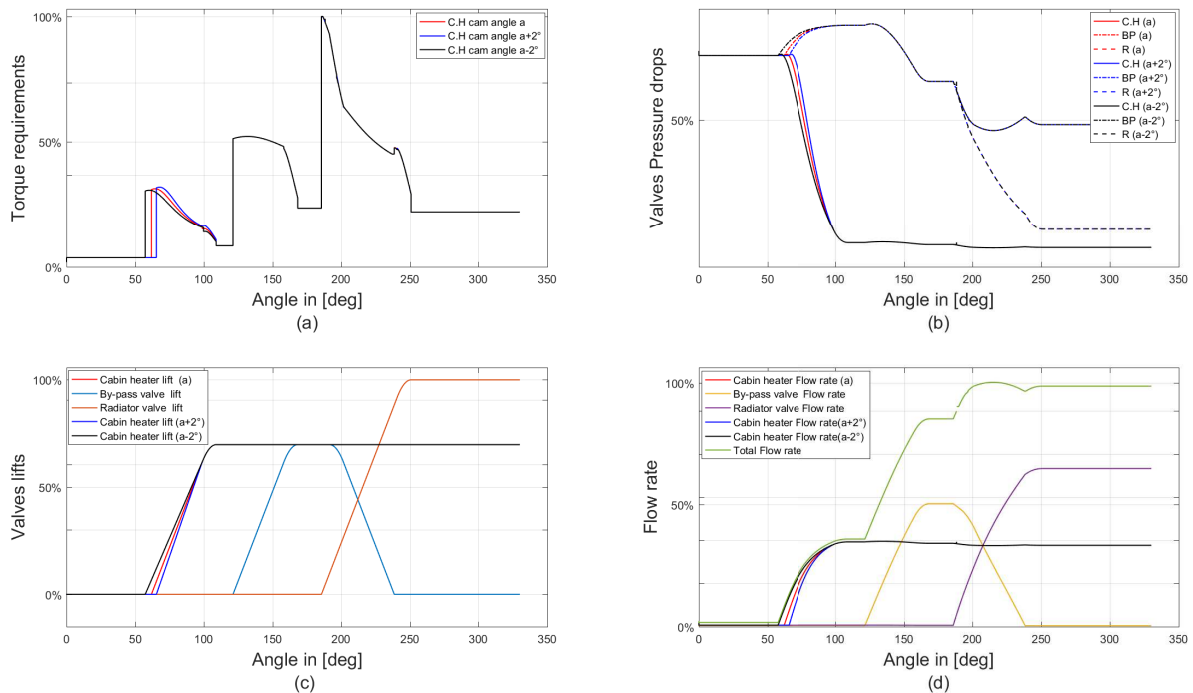


Figure 7: (a) resistive torque, (b) pressure drop, (c) lift and (d) flow rate sensitivity to raising angle variation ( $\pm 2$  degrees)

make a solid step in the the optimization process. The total resistive torque sensitivity analysis carried out above conduct basically to experimental validation tests of the model.

### 3 The Experimental validation of the model

#### 3.1 Experimental bench

The experimental bench was designed and then build in order to demonstrate experimentally the capacity of the multi-physical global model to predict accurate new designs suggestions. The hypothesis of the experimental protocol states that the numerical simulation is sufficiently accurate to help choosing a new geometrical configuration and a more robust design based on a sensitivity analysis of several parameters. The experimental bench emulates the operational mechanical aspects of the system for a single valve on its track (Figure 8.a). The test cam (Figure 8.b) numbered (6) is driven by an electrical brush-less motor (8) with a constant velocity of 0.5 rotation per minute. Torque measurements are obtained using a torque transducer (7), mounted on the cam shaft. Lift measurements are obtained using a laser position sensor (2), that reads indirectly the valve head vertical position. The mass loads are used to emulate a constant hydraulic pressure on the valve. In this section, third track test results are presented, it is designed to demonstrate the sensitivity of the torque requirement to angular and curves variation during the rising phase and the sliding down phase (Figure 9).

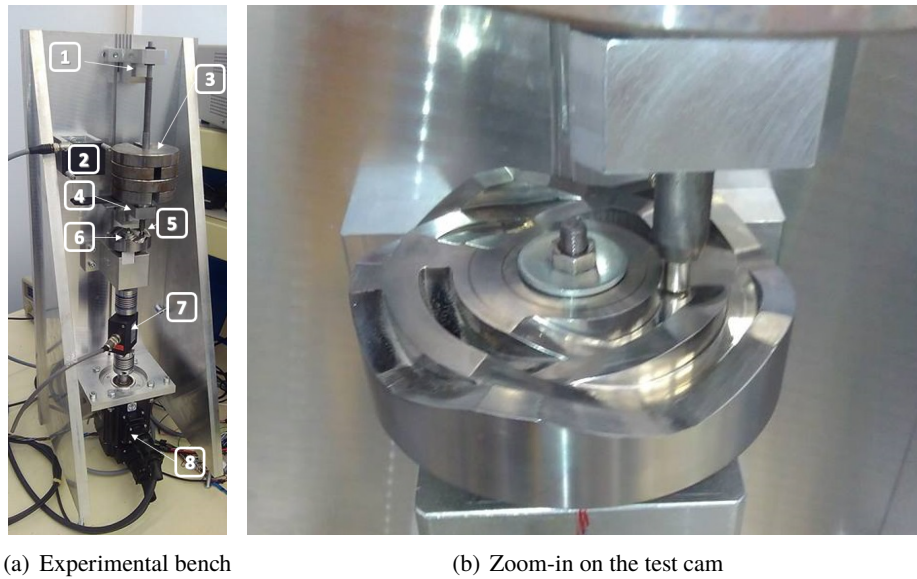


Figure 8: Experimental bench used to validate the model: (1) 2nd mass support, (2) Distance sensor, (3) Mass load, (4) 1st mass support, (5) Valve head, (6) test cam with 5 tracks, (7) Torque transducer, (8) Electrical motor

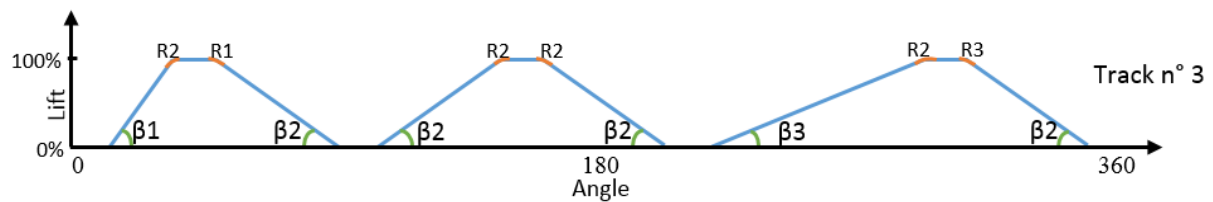


Figure 9: The test cam profile of the third track. (i)  $R_1$ ,  $R_2$  and  $R_3$  are curve radii ( $R_1 < R_2 < R_3$ ), (ii)  $\beta_1$ ,  $\beta_2$  and  $\beta_3$ : the cam rising angles ( $\beta_3 < \beta_2 < \beta_1$  and:  $\beta_1 = 3 \times \beta_3$ ,  $\beta_2 = 2 \times \beta_3$ )

## 3.2 Experimental results

An identification phase of parameters has taken place, in which frictional coefficients and initial resistive torque with no load were identified.

The experiment was carried out first for one and then two mass loads at a constant rotational cam speed of 0.5 RPM in order to remain in a quasi-static mode to avoid the dynamic effects and the high accelerations generated at high rotational speed which may have an influence on the torque and lift measurements.

Experimental measurements were acquired using the National Instrument acquisition and control modules. Experimental data were processed using Matlab acquisition toolbox. Lift and torque measurement for a complete clockwise revolution are shown below on figure 10.

As the lift increases from 0% to 100%, the resistive torque is also increased and stays constant for the rising angular portion, it depends on the value of the rising angle. On the angular portions of 100% lift, the torque remains constant and has the same value for the 3 bumps. On the angular portions of the profile curves, there is a slight difference in the slope of the resistive torque while falling down to its minimal value.

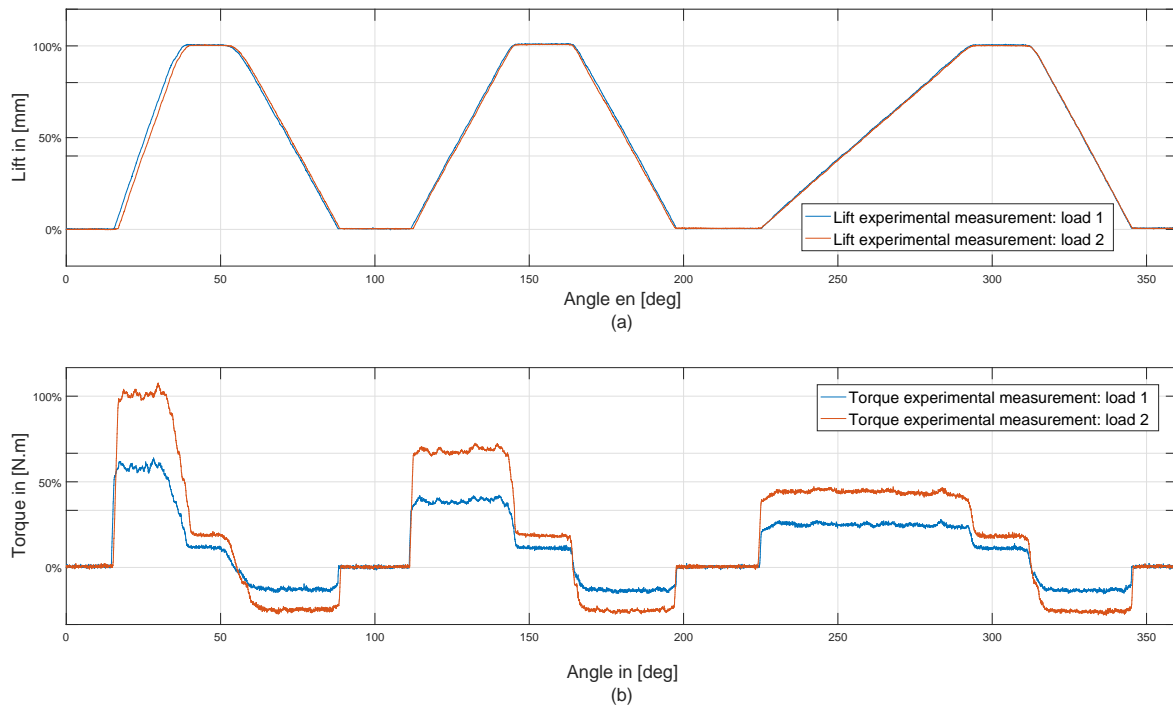


Figure 10: (a) Lift and (b) total resistive torque experimental measurements: the experiment was performed on the 3 track of the test cam for one mass load (blue), then two mass loads (orange), the cam rotational speed was set to 0.5 RPM

### 3.3 Experimental and numerical results comparison

In this section, the experimental measurements of total resistive torque and lift are compared to those obtained with the numerical simulations (Figure 11).

The error  $\varepsilon(\theta)$  between the numerical and experimental, normalized to the respective sensor accuracies, is presented on Figure 12 and is calculated as follows:

$$\varepsilon(\theta) = \frac{|X_{exp} - X_{num}|}{\Delta X_{accuracy}} \quad (1)$$

The error values which are less than one time the accuracy of the sensors could be considered as to be due to the sensor accuracy. For the values of error greater than many times the sensor accuracy, the mismatch could be considered to have geometrical and mechanical causes. One reason may be test cam manufacturing tolerances and uncertainties especially on the cam angles. The use of an elastic coupling may also lead to inaccurate measurement results. Lastly, the precision in the identification process of the frictional coefficient may also influence the error. In future works, a full 3D dimensional analysis of the manufactured test cam and valve head will take place in order to identify accurately the error sources.

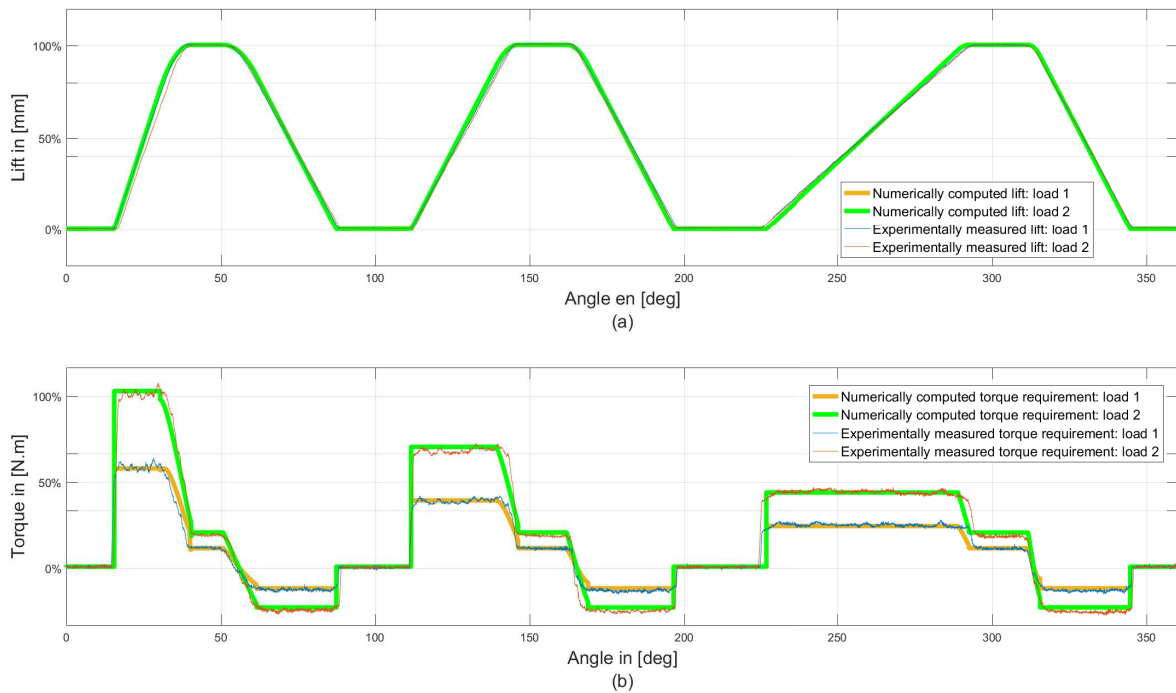


Figure 11: (a) Lift and (b) total resistive torque experimental measurements associated with numerical simulations of the lift and torque.

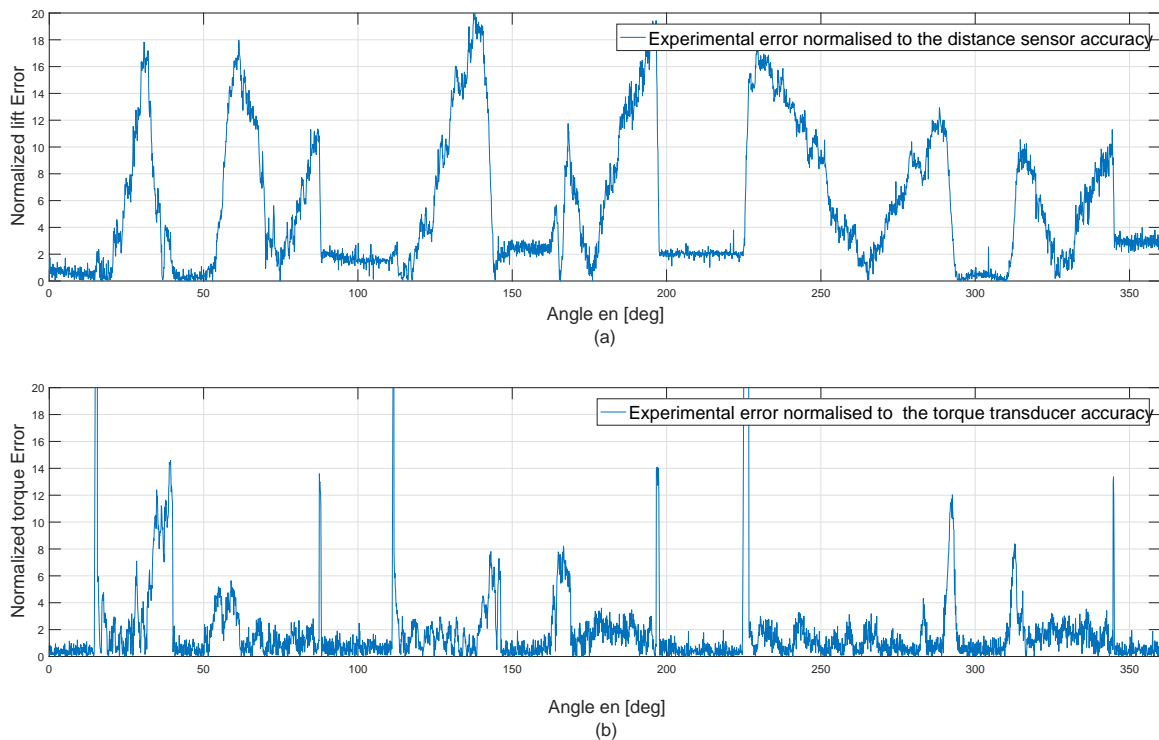


Figure 12: (a) Lift error and (b) torque error normalized to the respective sensors accuracies (calculated only for the first load). The calculated value of the root-mean-square error ( $\varepsilon_{rms}$ ) normalized to the torque transducer accuracy is  $\varepsilon_{rms_{torque}} = 4.19$ . The root-mean-square error normalized to the lift sensor accuracy is  $\varepsilon_{rms_{lift}} = 8.1$ .

A quadratic mean of the normalized error is also given in the caption of the Figure 12. These measure gives a global representation of the error over the profile and is calculated as follows:

$$\varepsilon_{rms} = \sqrt{\frac{1}{N_{points}} \sum_{i=1}^{N_{points}} \left( \frac{X_{exp} - X_{num}}{\Delta X_{accuracy}} \right)^2} \quad (2)$$

where:

$\varepsilon_{rms}$  : quadratic mean of the normalized error

$X_{exp}$  : experimental measurements

$X_{num}$  : numerical computations

$N_{points}$  : measurement points number

$\Delta X_{accuracy}$  : the sensor accuracy

## 4 Design optimization of the ACT valve

### 4.1 Introduction

Due to the complexity of the multi-physical global model and to the enormous time that the simulation in a closed loop optimization might take using the global model (up to 100 000 iterations). A simpler model has been created, in which certain functional aspects of the valve were neglected, such as wear on the heads of the valves, contact, clearances, curved surfaces, and valves geometry.

The determination of a geometric configuration of the ACT-Valve must meet a number of constraints. Moreover, this geometry strongly influences the torque requirement of the DC motor. This geometry is controlled by many parameters (as demonstrated in the sensitivity analysis) and it is difficult to find by hand the configuration that meets both the specifications while minimizing the torque requirements.

The ACT Valve current design complies with customer specifications. However, it is possible to find other geometrical configurations that require a lower torque on the DC actuator. To find these other configurations, we propose to solve this problem as an optimization problem.

The optimal geometrical configuration found after running the optimization loop needs to be tested in the multi-physical global model and results of the simulation are to be shown in future works.

Here a case of an ACT valve with three branches is presented: Cabin Heater, Radiator, and By-Pass circuits.

### 4.2 Optimization problem

An optimization problem is defined by its variables, constraints and objective functions. Here, only the cam geometrical parameters are considered as optimization variables. The optimization constraints and objective functions are defined below.

#### 4.2.1 Optimization variables : Cam geometry

The considered geometrical parametrization of the cam is represented in Figure 13.

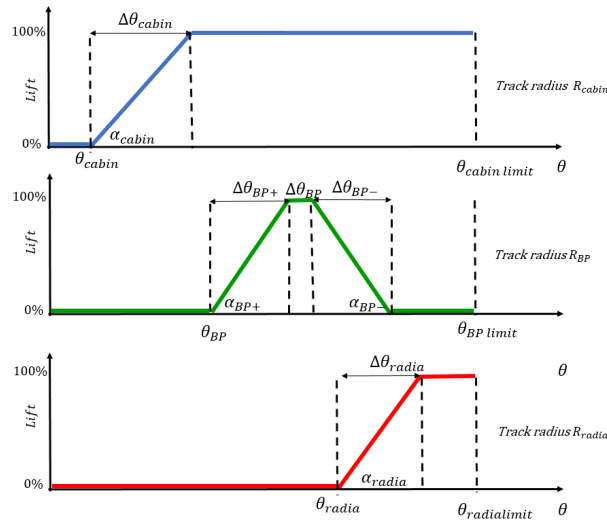


Figure 13: Cabine heater, By-pass and Radiator valves cam track profiles

It corresponds to the following variables :

#### a) Cabin heater track

Track radius  $R_{cabin} = [R_{cabinmin}..R_{cabinmax}]$

Angular position of start of climb  $\theta_{cabin} = [\theta_{cabinmin}..theta_{cabinmax}]$

Slope of climb  $\alpha_{cabin} = [\alpha_{cabinmin}..alpha_{cabinmax}]$

Angular range of the positive slope portion  $\Delta\theta_{cabin} = [\Delta\theta_{cabinmin}..Delta\theta_{cabinmax}]$

Angular limitation  $\theta_{cabinlimit}$

#### b) By-pass track

Track radius  $R_{BP} = [R_{BPmin}..R_{BPmax}]$

Angular position of start of climb  $\theta_{BP} = [\theta_{BPmin}..theta_{BPmax}]$

Positive slope of the climb  $\alpha_{BP+} = [\alpha_{BP+min}..alpha_{BP+max}]$

negative slope of the climb  $\alpha_{BP-} = [\alpha_{BP-min}..alpha_{BP-max}]$

Angular range of the full opening  $\Delta\theta_{BP} = [\Delta\theta_{BPmin}..Delta\theta_{BPmax}]$

Angular range of the positive slope portion  $\Delta\theta_{BP+} = [\Delta\theta_{BP+min}..Delta\theta_{BP+max}]$

Angular range of the negative slope portion  $\Delta\theta_{BP-} = [\Delta\theta_{BP-min}..Delta\theta_{BP-max}]$

Angular limitation  $\theta_{BPlimit}$

#### c) Radiator track

Track radius  $R_{radia} = [R_{radiamin}..R_{radiamax}]$

Angular position of start of climb  $\theta_{radia} = [\theta_{radiamin}..theta_{radiamax}]$

Slope of climb  $\alpha_{radia} = [\alpha_{radiamin}..alpha_{radiamax}]$

Angular range of the positive slope portion  $\Delta\theta_{radia} = [\Delta\theta_{radiamin}..Delta\theta_{radiamax}]$

Angular limitation  $\theta_{radialimit}$

### 4.2.2 Optimization constraints

The constraints can be classified in two different categories

#### a) Geometric constraints

The cam must have a sufficiently wide angular portion during which all valves will be closed:

$$\theta_{cabinmin} \geq S_1 \quad (3)$$

The cam must have a sufficiently wide angular portion during which the cabine valve is fully open and the other valves remain totally closed:

$$\theta_{cabin} + \Delta\theta_{cabin} + S_2 < \theta_{BP} \quad (4)$$

The lowest track radius must remain above a minimum radius value, due to the assembly solution:

$$(R_{cabinmin}, R_{BPmin}, R_{radiamin}) \geq S_3 \quad (5)$$

Track radius must be at least at a certain distance apart.

$$R_i - R_j \geq S_4 \quad (6)$$

where

$i, j$ : [cabin, BP, radia],  $i \neq j$

The largest radius must remain less than a maximum radius value

$$R_{cabin, BP, radiamax} \leq S_5 \quad (7)$$

where  $S_i$  : Boundary parameter

This parameter is set to the maximal or the minimal value that respects the constraints listed above.

## b) Hydraulic constraints

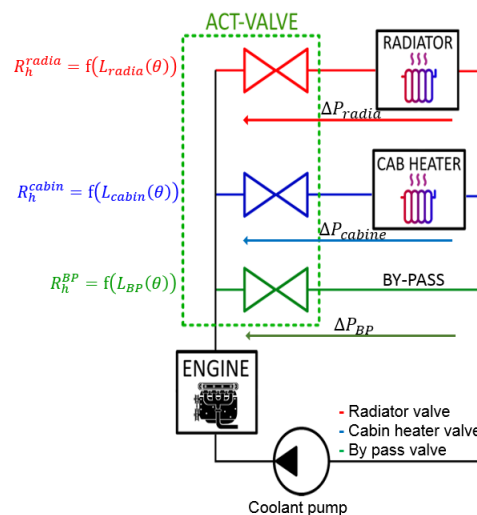


Figure 14: Cabine heater, By-pass and Radiator valves cam profil.

The hydraulic resistances of the valves in the fully open position must remain less than customer requirements:

$$(R_h^{cabin}, R_h^{BP}, R_h^{radia}) \leq CR_1 \quad (8)$$

The hydraulic resistance in the fully closed position must remain above a minimum value:

$$R_h^{closed} \geq CR_2 \quad (9)$$

where  $CR_i$  : customer requirements

### 4.2.3 Optimization objectives

#### a) Torque requirement minimization

As presented in [5], the total torque required is the minimal torque that the actuator must provide in order to rotate the cam. The torque depends on the angular position of the cam. It is the maximum value of this torque on a complete rotation of the cam that we are seeking to minimize.

$$C_{TOTAL}(\theta) = (\sum_i F_i(\theta) \times R_i \times [\tan(\alpha_i(\theta)) + f]) + C_B(\theta) + C_0 \quad (10)$$

with

$$F_i(\theta) = P_c + k \times L_i(\theta) + \Delta P_i(\theta) \times A_i \quad (11)$$

where

$C_{TOTAL}$ : total resistive torque

$F_i(\theta)$  : normal load due to the spring and the hydraulic forces

$i$  : [cabin heater, BP, radia]

$C_B$  : resistive torque created by the cam support plan

$C_0$  : Constant resistive torque created by the O ring seal

$R_i$  : valve track radius

$f$  : friction coefficient

$P_c$  : spring preloading

$k$  : spring stiffness

$\Delta P_i$  : pressure drops

$A_i$  : valve projected area

$\alpha_i$  : Slope of climb

$L_i$  : lift

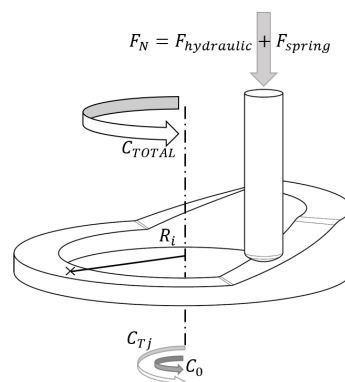


Figure 15: Total torque calculation schema:  $F_N$  vertical force applied on the contact point, including  $F_{spring}$  spring force and  $F_{hydraulic}$  hydraulic forces applied on the contact point (cam/valve)

**b) The packaging minimization (maximal occupied volume)** As a start, we chose to link the packaging requirement to the highest cam lift and to the maximum value of the largest track  $\max(R_i)$ . Therefore, it is this last value that we will also seek to minimize.

#### 4.2.4 Solving the optimization problem

As stated, this optimization problem is a bi-objective problem. We chose to solve it using a heuristic algorithm based on the particulate swarm method [16] adapted to treat bi-objective problems. This adaptation is inspired by [17] and has already been used in [18], [19] and well detailed in [15]. The size of the swarm has been set at 1000, and 500 iterations were chosen. To ensure a good convergence of our results, the process was run 10 times. The results discussed below.

### 4.3 Analysis and interpretation

After running the optimization algorithm 10 times, it proposed several geometrical configurations to reduce the torque requirements on the DC-actuator and it converges towards an optimal solution which results will be presented in this paper. The optimization algorithm presents a new geometrical configuration as it changes the initial parameters of the cam and the arrangement of its tracks (Figure 16.c).

In fact, it has reduced the cabin heater lift by 17% and put it on the second cam track. It also reduced the bypass lift by 9%, reduced the first slope by 17%, increased the second one by 25% and put the By-pass configuration on the third track. Finally, it proposed to reduce the radiator lift by 33%, the radiator slope by 32% and put it on the first cam track (Figure 16.b).

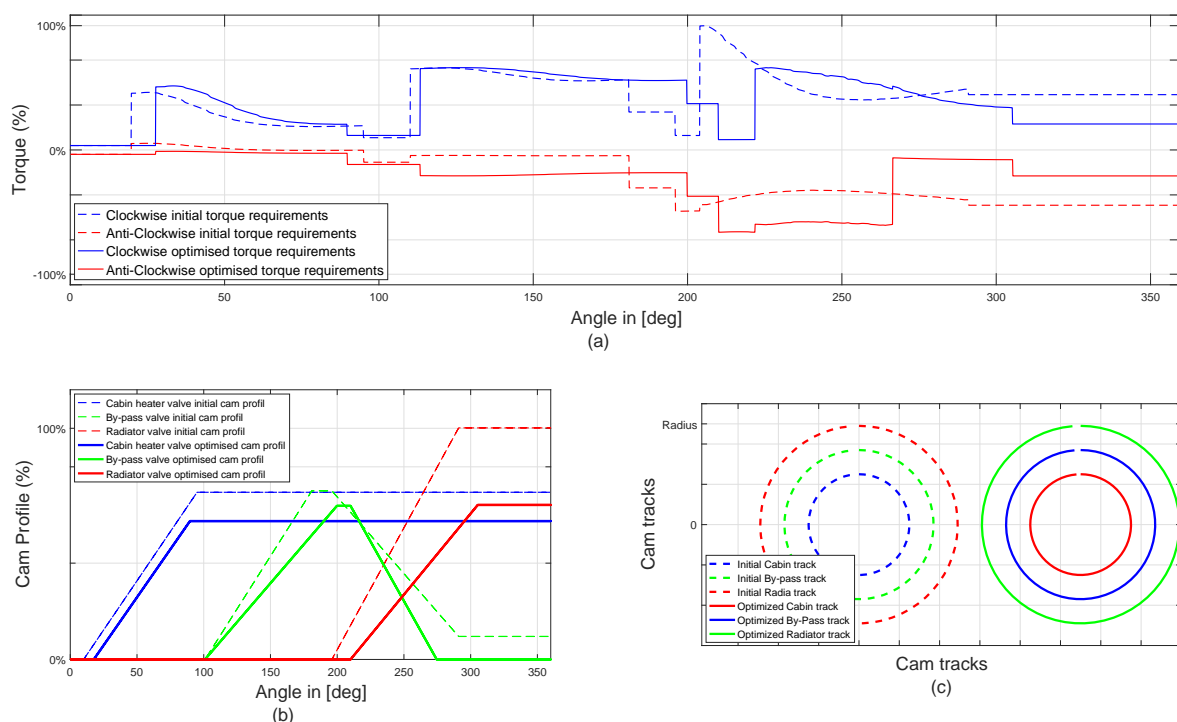


Figure 16: Results of the optimization algorithm: (a) initial and optimized torque requirements, (b) initial and optimized cam profile, (c) initial and optimized tracks arrangement

These changes caused a significant decrease of the torque requirements on the DC-actuator, 34% reduction on the maximum torque requirements (Figure 16.a) and about 33% reduction in cam packaging, this represents a 5% decrease in the total height of the ACT valve.

This new geometric suggestion proposed by the optimization algorithm constitutes a first step in the resizing the electrical actuator. The next step will be to implement this configuration on the global multi-physical model then to test it experimentally to validate this optimization and justify the probable actuator resizing.

## 5 Conclusion

This work helped to ensure the effectiveness and reliability of this valve over its lifetime, first by developing a multi-physical core model able to predict and simulate the operational aspects of the ACT valve then by optimizing the geometrical cam configuration on a simpler model in order to predict new design suggestions based on a particle swarm based optimization (PSO) loop. The suggestions of the optimization algorithm has brought a 34% reduction in the maximum torque requirement and about 5% of packaging in the cam direction. The next step will be to evaluate experimentally the geometrical configuration recommendations of the optimization algorithm then to seek ways to integrate these new configurations in the design process. Only cam optimization results were presented in this paper. In future works, the optimization will include other valve geometrical parameters. Another focus will remain on the identification of the error sources of the experimental bench, in this context, a 3D dimensional analysis of the test cam and the valve head are already scheduled to check the conformity of the manufactured test cam.

## References

- [1] Brent, North Sea and West, Forecast and Intermediate, Texas and Prices, Market and Report, Uncertainty and July, On and Nations, United and Council, Security and States, United and Union, European, August 2015 Short-Term Energy Outlook ( STEO ) 2016.
- [2] Commission européenne, "Règlement (UE) 2016/646," J. Off. l'Union Eur., vol. 3, 2016.
- [3] C. Rouaud, D. Gerard, B. Issartel, S. Pfeffer, S. Grolet, Thermal management solutions for Diesel engine, SIA publication, 28/05/2008.
- [4] M. Cormerais, T. Marimbordes, S. Warnery, D. Chalet and H. Mezher, "ACT Valve:Active Cooling Thermomanagement Valve", SAE Technical Paper 2014-01-0632, 2014, doi:10.4271/2014-01-0632.
- [5] M. Khammassi, T. Marimbordes, J. Aubry, B. Barbedette, M. Cormerais, C. LAROUCI, Q. FORSSARD, "A Multi-Physical Model of an Active Thermal Management Valve with Experimental Validation," SAE Technical Paper 2016-01-0180, 2016, doi:10.4271/2016-01-0180.
- [6] W.Nessim, F. Zhang., Z. CHanglu, Z. Zhenxia., "A Simulation Study of an Advanced Thermal Management System for Heavy Duty Diesel Engines", Proceedings of 2012 International Conference on Mechanical Engineering and Material Science (MEMS 2012).
- [7] Bosch,"Engine cooling". Automotive Handbook (3rd ed.). 1993. p. 413. ISBN 0-8376-0330-7.

- [8] “SimMechanics Contact Forces Library”, Updated 15 Sep 2015, <http://www.mathworks.com/matlabcentral/fileexchange/47417-simmechanics-contact-forces-library>.
- [9] P.Flores, J. Ambrósio, J P. Claro, & H. M. Lankarani, Kinematics and dynamics of multibody systems with imperfect joints: models and case studies, (Vol. 34). Springer Science & Business Media (2008).
- [10] HM. Lankarani, Nikravesh PEX. “A Contact Force Model with Hysteresis Damping for Impact Analysis of Multibody Systems”, *AMSE Journal of Mechanical Design*, 1990, 112, 369–376.
- [11] V. Hegadekatte, N. Huber, O. Kraft, “Modeling and simulation of wear in a pin on disc tribometer”, *Tribology Letters*, Vol. 24, No. 1, October 2006.
- [12] Archard, J.F. "Contact and Rubbing of Flat Surface". *Journal of Applied Physics* 24 (8): 981–988. doi:10.1063/1.1721448. (1953).
- [13] M. Guillon, J.P. Blondel, "Transmission de puissance hydraulique et pneumatique", *Techniques de l'ingénieur*.
- [14] Y. Shaoqiang, L. Zhong and L. Xingshan, "Modeling and simulation of robot based on Matlab/SimMechanics," 2008 27th Chinese Control Conference, Kunming, 2008, pp. 161-165.
- [15] M.Lossec, B.Multon & H.B Ahmed, Sizing optimization of a thermoelectric generator set with heatsink for harvesting human body heat. *Energy Conversion and Management*, 68, 260-265 (2013).
- [16] R. Eberhart and J. Kennedy, "A new optimizer using particle swarm theory" in MHS'95. Proceedings of the Sixth International Symposium on Micro Machine and Human Science, 1995, pp. 39–43.
- [17] C. a. Coello and M. Reyes-Sierra, "Multi-Objective Particle Swarm Optimizers: A Survey of the State-of-the-Art" *International Journal of Computational Intelligence Research*, vol. 2, no. 3, pp. 287–308, 2006.
- [18] J. Aubry, H. B. Ahmed, B. Multon, "Sizing Optimization Methodology of a Surface Permanent Magnet Machine-Converter System over a Torque-Speed Operating Profile: Application to a Wave Energy Converter", *IEEE Transactions on Industrial Electronics, Institute of Electrical and Electronics Engineers*, 2011, pp.1-1.
- [19] O. AYADI, et M. BARKALLAH, "An adapted particle swarm optimization approach for a 2D guillotine cutting stock problem", *Mechanics & Industry*, 2016, vol. 17, no 5, p. 508.J.
- [20] U. Asif, & J. Iqbal, Design and Simulation of a Biologically Inspired Hexapod Robot using SimMechanics,“. In Proceedings of the IASTED International Conference, Robotics (Robo 2010) pp. 128-135.(2010).